Hydrated elastin: Dynamics of water and protein followed by dielectric spectroscopies

V. Samouillan *, D. Tintar, C. Lacabanne

Physique des Polymères, Institut Carnot – CIRIMAT UMR 5085, Université Paul Sabatier, 31062 Toulouse Cedex 04, France

Keywords:
Elastin
Dielectric relaxations
Thermal analysis
Protein dynamics
Hydration shell
Hydrogen bonds

A B S T R A C T

The dielectric properties of elastin were investigated at different levels of hydration and specifically at the limit of freezable water apparition. The quantification of freezable water was performed by Differential Scanning Calorimetry (DSC). Two dielectric techniques were used to explore the dipolar relaxations of hydrated elastin: dynamic dielectric spectroscopy (DDS), performed isothermally with the frequency varying from 10^{-2} to $3 \cdot 10^{6}$ Hz, and the technique of thermally stimulated depolarization currents (TSDC), an isochronal spectrometry running at variable temperature, analogous to a low frequency spectroscopy (10^{-3}–10^{-2} Hz). A complex relaxation map was evidenced by the two techniques. Assignments for the different processes can be proposed by the combination of DDS and TSDC experiments and the determination of the activation parameters of the relaxation times. As already observed for globular proteins, the concept of ''solvent-slaved'' protein motions is checked for the fibrillar hydrated elastin.

1. Introduction

Protein surface hydration is essential to its structural stability and flexibility and protein associated water is often an integral element in biological activities [1,2]. The relaxation dynamics of hydration water in proteins is believed to control important dynamics of the proteins themselves [3]. Protein function usually involves protein motions corresponding to transitions between conformational states. Nevertheless, a complete understanding of the underlying coupling of proteins and water motions is still lacking [4].

For a series of globular proteins, the protein dynamics was proposed to be slaved [5–7] or plasticized by water dynamics, but the mechanism is still a subject of debate.

It has been suggested that the hydration shell and the surrounding bulk solvent have different effects on the protein motions. Fast β relaxations in the hydration would control fast local (β-like) fluctuations in the protein, whereas the cooperative α-relaxation in the bulk solvent would control the large-scale (α-like) protein motions [8]. It was also debated to what extent the slowdown of protein and water dynamics can be understood in terms of glass transition [9]. Some studies on hydrated proteins and more simple glass forming systems suggest that both the protein and the bound water participate in the glass transition mechanism [10]. In this case the relation between the secondary relaxation in the solvent and the conformation relaxation of the hydrated protein would be best described as symbiotic.

Connective tissues such as skin, lung, tendon and cardiovascular tissue are highly complex macromolecular materials. In addition to cellular components, the matrix contains fibers surrounded by a ground substance and water. The fibers are composed predominantly by fibrillar proteins, namely collagen and elastin [11]. Elastin can be considered as a three-dimensional network with 60–70 amino acids between two cross-linking points, conferring their extensibility to tissues [12]. It is noteworthy that elastin possesses a peculiar amino acid composition, with a great ratio of proline and glycine, driving a hydrophobic character for this protein [13]. The remarkable properties of hydrated elastin have aroused several studies to elucidate the structure–function relationship of this natural elastomer. This knowledge would be very important to understand the pathologies of elastic fibers, and to conceive new biomaterials with interesting elastic properties. Different recurring sequences of elastin were analyzed, through the synthesis and structure analysis of analogous polypeptides, or through molecular dynamics simulation, resulting in different models [14–19]. The Tamburro's model deals with isolated and labile β turns, resulting in a fluctuant polypeptide chain with chaotic motions in the relaxed state. The dynamic entropy of the system significantly decreases in the stretched and more structured state, and the classical theory of rubber elasticity can be applied to these sequences. Elastin can be described as a two-phase model consisting of hydrophilic cross-linking domains rich in lysine and alanine, and dynamic hydrophobic domains responsible for elasticity [20]. The

* Corresponding author. Address: Laboratoire de Physique des Polymères – CIRIMAT UMR 5085, Bat 3R1B2, 118, route de Narbonne – Université Paul Sabatier, 31062 Toulouse Cedex 04, France. Fax: +33 05 61 55 62 21.

E-mail address: vsamou@cict.fr (V. Samouillan).

doi:10.1016/j.chemphys.2011.04.016

hydrophobic domains can be described as a compact amorphous structure with fluctuating turns, buried hydrophobic residues and main-chain polar atoms forming hydrogen bonds with water. The determinant role of water must not be forgotten in the phenomenon of elasticity, since water makes elastin extremely dynamic in its relaxed state [14,20].

Dielectric techniques are useful to scan the dynamics of proteins [2–4,6,21]. In a previous study [22] we investigated the chain dynamics of dehydrated elastin in the nanometer range by DSC and dielectric techniques (DDS/TSDC). We showed in that case that dry elastin possessed the peculiar features of a fragile liquid, associated with the strength and nature of interactions. We also investigated hydrated elastin by DSC and TSDC in the native state, namely for high degrees of hydration (typically 50% of hydration) and we could propose assignment for the different dipolar processes [23]; nevertheless, the strong answer of ice can induce perturbation to explore more in detail the dynamics of the hydration shell of the protein.

More recently, DDS experiments on deeply supercooled hydration water in elastin and collagen showed that the dynamics of the hydration layer was influenced by the protein surface motion [24]. Moreover, the combination of DDS and ^{2}H/13C NMR experiments on hydrated elastin and collagen attempted to precisely assign the relaxation modes of the hydration layer [4,9] to specific water motions. The combined motions of water and peculiar soluble sequences of elastin (reductionist approach) were also followed by DDS in solution and gave information on the mutual influence between solvent and peptide, clearly showing that peptides conformations and molecular mobility are correlated to the solvent, but also that solvent is conditioned by peptide [25]. In the present study we use the global approach to study elastin: first we propose to detect accurately the apparition of free water in the insoluble elastin/water system, and second we propose to compare the dynamics of elastin for different levels of hydration, in order to scan the mobility of elastin and water from the hydration shell of the protein. Another aim will be to check if bound water alone is sufficient to assure protein mobility and consequently protein function.

2. Experimental

2.1. Materials

Insoluble elastin was purified from bovine ligament neck by the Lansing's method [26] and was shown by amino acid analysis to be free of microfibrillar proteins. It was freeze-dried and powdered into grains with diameter < 130 μm. After complete dehydration under P_2O_5 overnight at 105 °C, elastin was rehydrated with deionized water (resistivity equal to 18 MΩ cm). The hydration level h is defined as the mass of water divided by the mass of dry elastin and was adjusted between 0.1 and 2 for further analyses.

2.2. Differential Scanning Calorimetry (DSC)

DSC thermograms were recorded with a Differential Calorimeter DSC2920 from TA Instrument. The temperature and power scales were calibrated using the manufacturer's instructions with cyclohexane and indium as ICTA standards. Samples 5–10 mg were sealed into hermetic stainless steel pans and empty pans were used as references. After cooling at −30 °C at 10 °C/min and 5 min equilibrium, scans were performed from −30 to 40 °C at 5 °C/min.

2.3. Dielectric analysis

2.3.1. Dynamic dielectric spectroscopy (DDS)

The dielectric measurements were performed on a broad-band dielectric spectrometer BDS 4000 system from Novocontrol. Samples were kept in a special cell usually devoted to hydrated samples consisting of two stainless steel electrodes surrounded by a Teflon ring. The diameter of the electrodes was 10 mm, and the thickness of the samples was 0.2 mm. A blocking electrode (Teflon® film, 10 μm thick) was placed between the sample and the upper electrode in order to reduce the large contribution of electrode polarization to the spectra at low frequency and to suppress the parasite conduction, as already performed by some workers [6,38].

Isothermal measurements of the complex dielectric function $\varepsilon^* = \varepsilon' - i\varepsilon''$ were performed at every fifth degree, with an isothermal stability of ±0.1 °C, in the frequency range 10^{-2} to $3 \cdot 10^6$. The experimental limit for the loss factor ($\tan\delta = \varepsilon''/\varepsilon'$) was about 10^{-4}.

2.3.2. Thermally Stimulated Depolarization Currents (TSDC)

Thermally stimulated currents measurements were carried out with a dielectric apparatus developed in our laboratory and previously described [27]. Samples were placed between two stainless steel electrodes surrounded by a Teflon ring. Measurements were performed with and without a blocking electrode consisting in a Teflon® film, 10 μm thick. Before experiments the cryostat was flushed and filled with dry He to insure good thermal exchanges. To record complex spectra, the sample was polarized with a static electric field E_p at a given polarization temperature T_p for a time t_p which is long enough so that the polarization reached equilibrium. Then the sample was quenched by a cooling process to $T_0 \ll T_p$, allowing the orientation polarization $P(T_p)$ to be frozen-in. Finally the electric field was cut off and the sample was short-circuited for a time t_{cc} long enough to remove fast relaxing surface charges and to stabilize the sample temperature. The capacitor was then connected to a very sensitive electrometer (Keithley 642, 10^{-16} A accuracy). The depolarization current $I(T)$ induced by the linear increase of temperature ($T = qt + T_0$) was subsequently recorded versus temperature, giving the relaxation spectrum of the sample. In the present study, the polarization conditions resulting in reproducible dipolar relaxations were as follows: T_p = 0 °C, t_p = 2 min, E_p = 600 V/mm, t_{cc} = 2 min and q = 7 °C/min.

The TSC spectra of hydrated elastin obtained from this procedure are complex, arising from a distribution of relaxing entities. In order to resolve experimentally these spectra in a series of elementary depolarizations, the technique of Fractional Polarizations (FP) was applied. For this investigation, the sample was only polarized within a narrow temperature window ΔT during the cooling process, and the depolarization current was recorded as previously indicated. In the present work a value of 5 °C was used for the interval of fractional polarizations. By shifting the ΔT polarization window by steps of 5 °C in the temperature range of the complex relaxation modes, a set of elementary processes was obtained.

3. Results and discussion

3.1. Detection of freezable water in hydrated elastin

Thermograms of elastin hydrated between h = 0.22 and h = 1 are reported in Fig. 1. An endothermic peak with a maximum at −2 °C, with an intensity varying with the hydration level is observed for highly hydrated elastins. This endothermic peak corresponds to the melting of freezable water [28,29] in the hydrated protein. Previous studies [23] showed that freezable water in hydrated elastin appears between h = 0.2 and h = 0.3. Here we carefully looked for this limit, which is comprised between h = 0.25 and h = 0.28 as observed in the enlarged zone. So we can assume that for elastin hydrated at h = 0.25 and below, there is only unfreezable water in the system. This value is in good agreement with literature values;

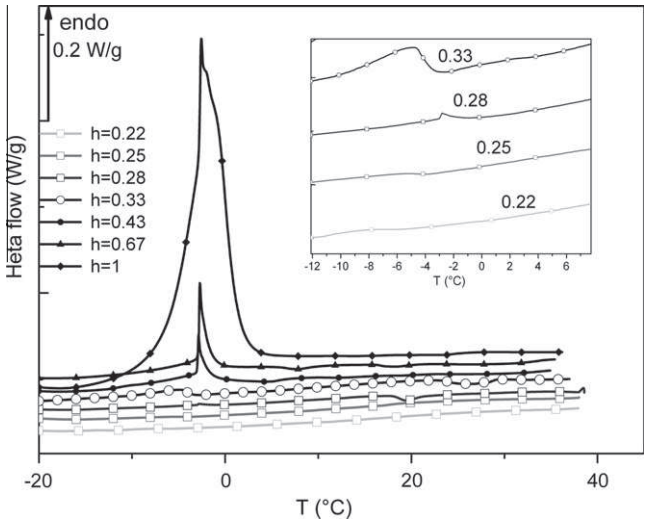

Fig. 1. DSC thermograms of elastin recorded between −30 and 40 °C at 5 °C/min for various hydration levels.

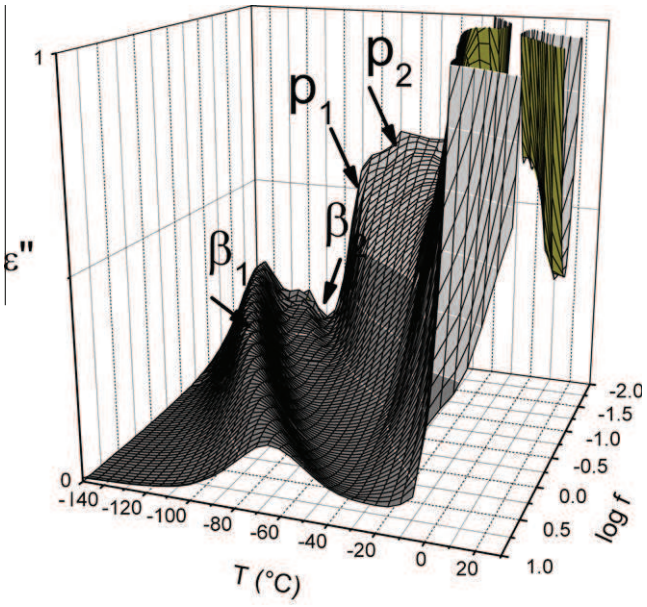

Fig. 2. Imaginary part (ε'') of the dielectric spectrum of hydrated elastin (h = 0.25) as a function of frequency and temperature.

usually about 0.3–0.7 g of bound water remains associated per gram of a "dry" protein [2]. In the case of elastin, one of the most hydrophobic proteins, the low value found is coherent. For h comprised between 0.25 and 0.28, a basic calculation – assuming that the average molar mass of one amino acid in elastin is 84 g/mol [30] – leads to the value of 1.2–1.3 molecule of water bound to one amino acid. These results are close to previous models on hydrated elastins, elaborated by analogy with polyamides/water systems [31]: for these authors, three molecules of water could be bound to two residues, the first one strongly bound to two carbonyl groups of elastin, the others more weakly bound, inserted between preexisting hydrogen bonds between carbonyl and amine groups. Similar results were obtained by solid state ^{13}C NMR on differently hydrated elastins, showing the existence of a first hydration layer, corresponding to a ≈30% hydration level of elastin [32]. As water is added, one plausible model might include an extensive network from peptide backbone to H_2O molecules in the first, second and subsequent hydration layers.

When $h > 0.25$, some water molecules can form hydrogen bonds among each others, initiating bulk water formation, i.e. freezable water. Interestingly, the physical properties of elastin exhibit a nearly identical relationship to hydration: namely, samples with 40–100% hydration have rubber-like characteristics of flexibility and elasticity, whereas samples with 0–30% hydration are brittle [32,33].

3.2. Elastin and water dynamics

3.2.1. Global dielectric relaxations

The reel and imaginary parts of the complex permittivity of differently hydrated elastins from DDS experiments were measured from −150 to 30 °C. In Fig. 2, the three-dimensional representation of the dielectric loss, i.e., the imaginary part of the dielectric function ε'' versus frequency and temperature is shown for elastin hydrated at h = 0.25. The dielectric spectrum can be described by several processes, both relaxations, which give rise peaks in the spectrum, and polarization effects or conductivity, which both cause an increase of ε'' at low frequencies. For more convenience, we have plotted in Fig. 3 selected isochronal dielectric losses (ε'') versus temperature for elastin hydrated at h = 0.25. The four relaxation modes have been labeled β1, β2, p1 and p2 in the order of decreasing frequency at constant temperature (Fig. 2), or in the order of increasing temperature at constant frequency (Fig. 3), by analogy with previous dielectric studies on other hydrated proteins [6,34].

The imaginary and real parts of the dielectric spectra of differently hydrated elastins were fitted using the well-known Havriliak–Negami (HN) functional form [35]:

$$\varepsilon^* = \varepsilon_\infty + \frac{\varepsilon_0 - \varepsilon_\infty}{[1 + (i\omega\tau_{HN})^\alpha]^\beta} \quad (1)$$

where α and β are the spectral shape parameters, τ_{HN} the average relaxation time, ε_0 and ε_∞ the limits of the dielectric permittivity at null and infinite frequencies obtained from the fits.

Decomposition of the loss spectra into individual processes was accomplished using several HN functions (in general, 2 HN functions) and a conductivity term ($\sigma_0/i\omega_0$) when needed. In a general way, the different loss peaks were sufficiently distinct so that the maximum of each peak was observable. There is a highly controversial discussion whether advantages or disadvantages when

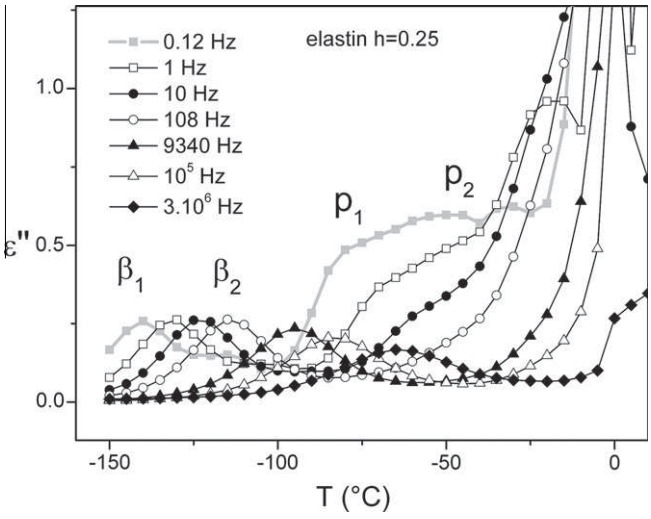

Fig. 3. Dielectric losses (ε'') of hydrated elastin (h = 0.25) as a function of temperature for selected frequencies.

using blocking electrodes in dielectric studies on systems showing substantial conductivity. As a matter of fact, a Maxwell–Wagner polarization may arise. If so, the slowest process ($p4$) might not be due to protein motions.

Since TSDC generally allows a good resolution of relaxation processes, due to its very low equivalent frequency, complementary information can be brought by this technique; the complex TSDC spectra of elastin hydrated at $h = 0.25$ (with and without using a blocking electrode) recorded after a polarization temperature of -5 °C are reported in Fig. 4. Without the use of a blocking electrode, two modes are observed at low temperature, located at -135 °C and -108 °C, respectively, and followed by a great increase of the intensity due to electrode polarization and/or conductivity. A mode is present as a shoulder between -75 °C and -70 °C. When a blocking electrode is used, the lower temperature mode remains quasi unchanged, but with the suppression of the parasite conductivity the third relaxation process is revealed as a peak at -60 °C. Reminding that the equivalent frequency of TSDC is close to 10^{-3} Hz in this temperature range [36], a good agreement is noticed between the TSDC spectrum of hydrated elastin ($h = 0.25$) and the isochrones extracted from DDS relaxation map reported in Fig. 3: the four processes β1, β2, p1 and p2 with increasing temperature at constant frequency are detected in both cases. As p1 is observed in TSDC without blocking electrode, it can be associated to a relaxation process. The dipolar character of $p4$ remains uncertain, since this mode is hidden under the conductivity when no blocking electrode is used.

Comparative studies on elastin at $h = 0.1$ showed that the blocking electrode did not induce additional process on the dielectric spectra [22,37]. Nevertheless, more hydrated elastin corresponds to a more complex system and artifacts can be brought by the use of a blocking electrode. That the reason why we must be cautious with the interpretation of high temperature modes, and mainly focus in this study on the fastest components β1 and β2 modes.

In Fig. 5 are plotted the dielectric losses (ε'') of elastin hydrated between $h = 0.1$ and $h = 2$ as a function of frequency for the isotherms $T = -100$ °C. As well described in literature data, these two relaxation processes are usually observed in hydrated polymers, biomolecules and small organic molecules in solution and associated with the water dynamics. As observed in literature data [6,9,38,39], this mode is symmetrically broadened ($\beta \approx 1$, $0.4 < \alpha < 0.5$), suggesting that it is due to a more local β-relaxation rather than the cooperative α-relaxation. The faster process (β_1) is known

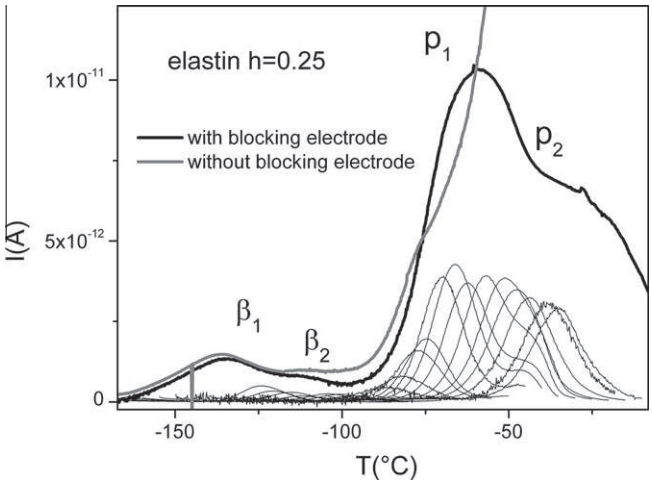

Fig. 4. Complex TSC spectrum of hydrated elastin ($h = 0.25$) for a polarization temperature $T_p = -5$ °C with and without the use of PTFE blocking electrode. Also reported are the corresponding elementary spectra obtained from the FP procedure.

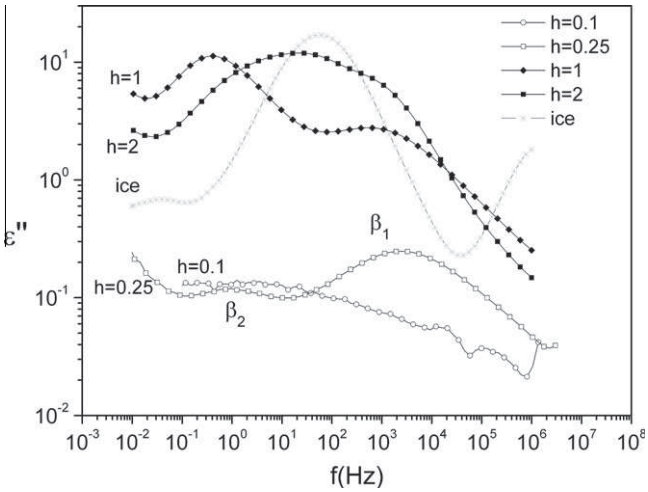

Fig. 5. Dielectric losses (ε'') of elastin for various hydration levels and ice (deionized water) as a function of frequency at $T = -100$ °C.

as the universal β relaxation in deeply supercooled confined water [9,10,34,39] and it is generally addressed to the reorientation of water molecules. The associated dielectric strength evidences that this reorientation is not assigned to pure solvent but to the hydration layer [24]. The β2 mode is also found symmetrically broadened (($\beta \approx 1$, $0.5 < \alpha < 0.75$) in the temperature domain where it is observable. The assignment of the slower process β2 is more ambiguous: the presence of a relaxation process in this temperature/frequency range is reported in literature data [39] for various systems hydrated between 30% and 50% (h between 0.4 and 2), and usually follows a Vogel–Fulcher–Tammann [41] dependence with temperature. It has been associated with the cooperative rearrangement of the whole system, i.e. the matrix (solute) plus water [39]. For others workers, this mode can follow an Arrhenius-like dependence and it could be attributed to local non cooperative motions of the proteins, probably polar side groups [6,34], or associated with a region of the protein where dominates tightly bound water [38]. In the case of collagen, a fibrillar protein from connective tissues, the β2 process only appears for hydration levels superior to 0.3 and was attributed to excess, freezable water [4,21]. To clarify the β2 mode origin in the case of hydrated elastin, we also plotted on Fig. 5 the dielectric loss (ε'') of pure de-ionized ice. We can observe that the β2 mode is present for the differently hydrated elastin, from $h = 0.1$ to *$h = 2$. For $h = 0.1$ to $h = 1$, the maximum of* β2 mode is comprised between 0.1 and 1 Hz, whereas the relaxation process of deionized ice is observed at higher frequencies. Moreover, we checked by DSC that elastin at $h = 0.1$ and $h = 0.25$ did not possess freezable water so the β2 mode observed in hydrated elastin ($h = 0.1$–1) was not be attributed to pure ice in this case. For $h = 1$, the dielectric answer of ice must be hidden by the β1 and β2 processes but its presence is testified by the translation of the ε'' curves toward high values. For elastin at $h = 2$, the three processes – the β1 mode, the β2 mode and the mode of pure ice – are observed in this frequency range, requiring in this case a fit by 3 HN functions. A similar behavior was found for hydrated bovine serum albumin [38]: the low temperature dielectric processes are readily distinguishable at low water content. However, with increasing water content, the processes evolve gradually into a broad spectrum at which point a physically meaningful separation of the overlapping processes is not possible.

3.2.2. Fast dynamics: β1 and β2 processes

3.2.2.1. Temperature dependence of the β1 mode. Fig. 6 shows the temperature dependence of the average relaxation time τ_{HN} for

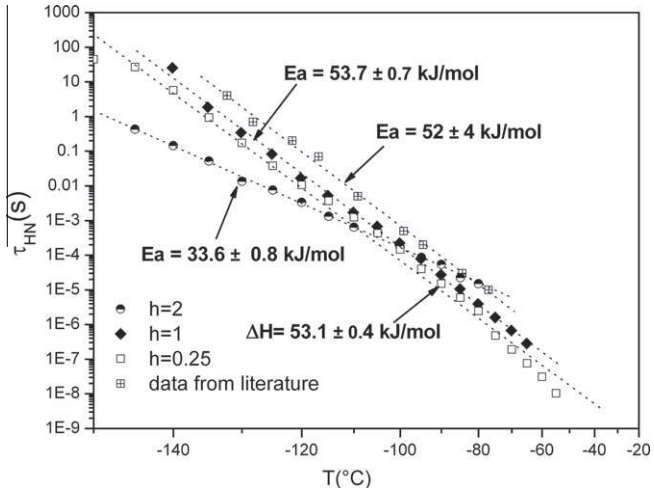

Fig. 6. Temperature dependence of the relaxation times τ_{HN} for the $\beta 1$ process of elastin for various hydration levels. Also reported are the relaxation times τ_{HN} for the $\beta 1$ process in hydrated organic molecules from literature data [35].

the fastest process, namely the β_1 mode, for elastin hydrated between $h = 0.25$ and $h = 2$ (for $h = 0.1$, the β_1 mode is not detectable). Also superimposed are the temperature dependence of $\tau_{HN\beta 1}$ for a large class of hydrated organic molecules ($h = 0.4$–1) from literature data [39]. For the differently hydrated elastin, an Arrhenius-like behavior is found as already observed in literature data in the same scale of hydration [9], without any transition to a VTF behavior. The activation energies obtained from a linear fit are close to 53 kJ/mol (except for $h = 2$, with $Ea = 33.6$ kJ/mol), and the preexponential factors $\tau 0$ comprised between 10^{-20} and 10^{-21} s. These values are very similar to values from literature including a wide range of hydrated materials [3,24,38,40]. As the enthalpy of hydrogen bonds in ice I was estimated at −23 kJ/mol [42], the values of *Ea* roughly correspond to the energy needed for the breaking of two hydrogen bonds [24,40]. As already observed [9,39,43], the value of *Ea* is significantly larger than 46 kJ/mol, and this increase was interpreted as the self-association of water molecules in hydrophilic solutions [39]. In our case, elastin is insoluble and considered as a hydrophobic protein when compared to others proteins. Nevertheless, from a chemical point of view its ability to form hydrogen bonds with water confers a hydrophilic behavior. So the $\beta 1$ mode of hydrated elastin, as previously assigned in literature for others materials, is associated with the reorientation of water molecules in the hydration shell of elastin. A recent study by ^{2}H NMR spin–lattice relaxation showed a nice agreement with the results of the dielectric process $\beta 1$ for elastin, collagen and myoglobin hydrated between $h = 0.25$ and 0.43, indicating that the same dynamical process is probed by DDS and NMR [4,9]. The NMR data indicate that the reorientation of water molecules in the hydration layer involves large jump angles, most probably distorted tetrahedral jumps, differing from a rotational diffusion, without excluding that the tetrahedral jump motion is governed by the protein surface. The $\beta 1$ mode allows following the dynamics of hydrogen bonds network in the hydration layer of elastin.

For higher degrees of hydration ($h = 2$), the activation energy of the $\beta 1$ mode is lower. In this case, free water constitutes 87.5% of the whole water and must influence the dynamics of the hydration layer, with an increasing gradient between closely bound water and loosely bound water. In this case, the temperature dependence of the deionized ice relaxation mode can be followed and an Arrhenius-like dependence is found with an activation energy of 20.4 kJ/mol, in agreement with literature data for deionized or distilled water and saline solutions of low concentration [44–47].

3.2.2.2. Temperature dependence of the β2 mode. Fig. 7 shows the temperature dependence of the average relaxation time τ_{HN} of the β_2 mode for elastin hydrated between $h = 0.1$ and $h = 2$; also superimposed are the temperature dependence of the relaxation time of $\beta 2$ for hydrated proteins and organic molecules ($h = 0.2$ to 2) from literature data [6,9,34,38,39]. For elastin, an Arrhenius-like behavior is noted for the different hydration level, with average values of activation energies varying from 42 to 48 kJ/mol, and preexponential factors between 10^{-17}s and 10^{-14} s. For elastin at $h = 2$, as previously observed for the $\beta 1$ mode, the relaxation times τ_{HN} is lower, attesting a faster dynamics of the $\beta 2$ mode in this case. As for the $\beta 1$ mode, the activation energy is that required to break two hydrogen bonds. Nevertheless, we must be cautious on the origin of this $\beta 2$ mode: some workers observe a mode with a similar dynamics in collagen for $h > 0.3$ and attribute it to excess water [9,24]. For others, the $\beta 2$ mode observed in hydrated myoglobin, hemoglobin and albumin could be assigned to little cooperative reorientations in the system protein–water [6,34,38]. As reported on Fig. 7, the relaxation time of the $\beta 2$ mode of elastin in the scanned temperature range is intermediate between the relaxation mode associated to excess water [9,24] and the relaxation mode addressed to the localized motions of hydrated side groups on the proteins [6,34,38], preventing us from an unambiguous assignment. Nevertheless it can argued that even for a low hydration level ($h = 0.1$), the relaxation mode attributed to the $\beta 2$ one is detectable, with a similar dynamics as observed for higher hydration levels. So a low water content (9%) seems sufficient to initiate local motions in the protein (note that the $\beta 2$ mode is lacking for completely dehydrated elastin [48]. The fact is in good agreement with the CPMAS spectra of 0–30% hydrated elastins which are similar [32]. This indicates that the water coverage provides the flexibility needed for the biological activity of the protein [2]. Water helps in reducing the number of barriers in the free energy landscape.

3.2.2.3. Evaluation of β2 cooperativity. In order to get complementary information on the relaxation processes scanned by DDS, the fractional polarization (FP) method was applied to resolve experimentally the complex TDSC spectra of hydrated elastin into elementary spectra. The set of elementary spectra recorded by shifting the polarization window from −140 to −45 °C are reported in Fig. 4. Each elementary spectrum obtained by the FP method can

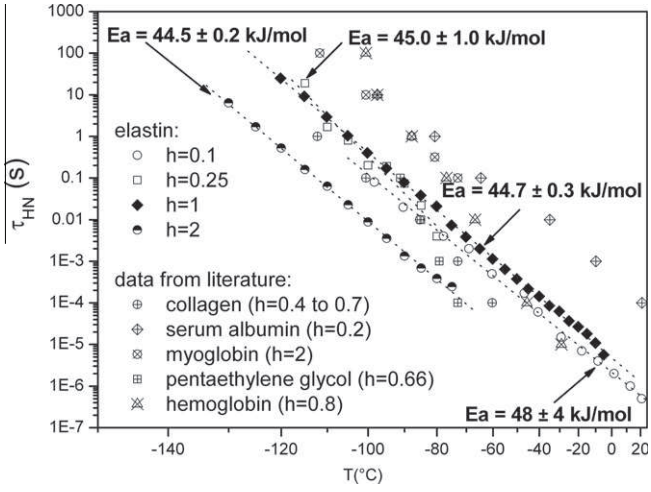

Fig. 7. Temperature dependence of the relaxation times τ_{HN} for the $\beta 2$ process of elastin for various hydration levels. Also reported are the relaxation times τ_{HN} for the $\beta 2$ process in collagen [9], serum albumin [38], myoglobin [34], hemoglobin [6] and pentaethylene glycol [39].

be considered as a Debye peak, and thus is associated with a single relaxation time $\tau(T)$. Using the Bucci–Fieschi's framework [49], the temperature dependence of $\tau(T)$ can be determined experimentally without any hypothesis on its temperature dependence, by the following relationship:

$$\tau(T) = -\frac{P(T)}{dP(T)/dt} = \frac{1}{qI(T)} \int_T^{T_f} I(T)dT \quad (2)$$

where $P(T)$ is the polarization, $I(T)$ is the depolarization current and T_f *the final temperature when* $I(T)$ returns to 0.

The elementary relaxation times $\tau(T)$ computed from each elementary spectrum are plotted versus the reciprocal temperature in Fig. 8. Since the origin of the p4 mode is uncertain and could be due to the use of a blocking electrode, we chose to superimpose on this figure the temperature dependence of τ_{HN} for elastin ($h = 0.25$) obtained from DDS measurements for the $\beta1$, $\beta2$ and p1 processes.

We notice that the temperature dependence of all the relaxation times isolated by the FP method obeys an Arrhenius–Eyring law:

$$\tau(T) = \frac{h}{kT} \exp\left(-\frac{\Delta S}{k}\right) \exp\left(\frac{\Delta H}{kT}\right) \quad (3)$$

where k is Boltzmann's constant, R the gas constant, h the Planck's constant, ΔH the activation enthalpy in J mol^{-1} and ΔS the activation entropy in J mol^{-1} K^{-1}. Note that the T^{-1} variation is negligible regarding the exponential term so that $\tau_0 = h(kT)^{-1} \exp(-\Delta S/R)$ is practically independent on temperature. Each elementary relaxation time is so characterized by the pre-exponential factor τ_0 and the activation enthalpy ΔH. For each elementary process of hydrated elastin ($h = 0.25$) are plotted the activation enthalpy ΔH versus the temperature of the peak in Fig. 9. A good agreement is observed between the temperature dependence of the relaxation times of the different relaxation processes scanned by TSDC and DDS in Fig. 9. The decomposition of the $\beta1$ mode is not accessible via TSDC (the experiment should be performed at lower temperature) but the $\beta2$ and p2 processes are observed in the different time scales according to DDS and TSDC scanning frequencies. The relaxation time τ_{HN} from DDS is a global relaxation time whereas the relaxation times from TSDC are elementary and give access to the experimental distribution.

The criterion of Starkweather [50] can be used to analyze the nature of the molecular mobility. To discriminate between cooperative processes, the Starkweather's function (continuous line) has been superimposed in Fig. 9. It corresponds to activation enthalpies derived from activated states theory at null activation entropy, and obeys the following law:

$$\Delta H_0 = RT \ln\left(\frac{kT}{2\pi h f_{eq}}\right), \quad (4)$$

where f_{eq} is the equivalent frequency of TSC (f_{eq} 10^{-3} Hz with our experimental conditions).

It can be observed from Fig. 9 that the lowest temperature process $\beta2$ obeys the null entropy prediction: this relaxation process can be considered as non- or little cooperative. Previously attributed by DDS to local motions in the elastin–water system, it reflects the movement of small molecular segments without modification of the environment. So it prevents us from addressing it to a delocalized motion.

3.2.2.4. Relation between β1 and β2 modes. As firstly showed by Fenimore et al. [5,7] on hydrated myoglobin, internal proteins motions would be slaved by the fluctuations in the hydration shell, while large scale proteins motions of protein would be slaved by the fluctuation of the bulk solvent. Others studies showed this coupling dynamics for hydrated proteins [34] or hydrated organic molecules [39]. At the present time, this kind of study has not been performed for a fibrillar protein such as elastin. We reported in Fig. 10 the variations of the relaxation time of the $\beta2$ mode versus the relaxation time of the $\beta1$ mode for elastin at $h = 0.25$, 1 and 2 in logarithmic scales. For the hydration levels $h = 0.25$ and $h = 1$, a direct power law is observed (slope of the line is 1) with $\tau_{HN\beta_2} \approx 10^3 \tau_{HN\beta_1}$. The relation is less direct for $h = 2$, because of the difficulty to extract properly the relaxation time of bound water in a system that contains 87.5% of bulk water.

So we can assume, as observed for globular proteins, that the model suggested by Fenimore is consistent for elastin: the dynamics of elastin/water local motions is driven by the dynamics of water molecules in the hydration shell, the $\beta1$ mode being a thousand fold faster than the $\beta2$ mode. This fact can be illustrated by a dynamic exchange between the different hydration layers around the protein, as suggested in different hydrated proteins models [1,2].

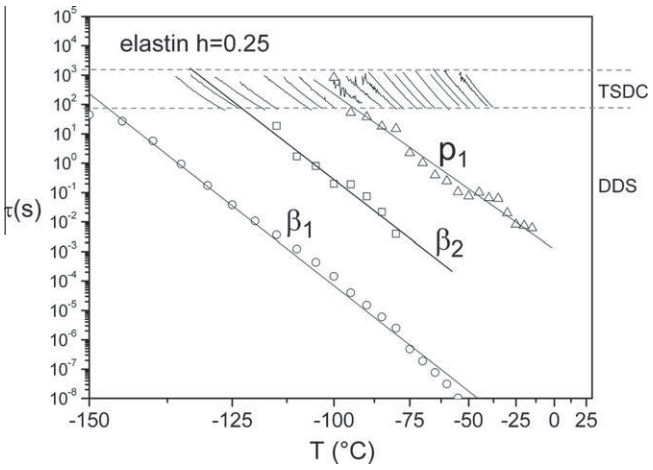

Fig. 8. Temperature dependence of the relaxation times τ_{HN} for the $\beta1$, $\beta2$, p1 and p2 processes of hydrated elastin ($h = 0.25$) from DDS experiments. Also shown are the temperature dependence of the elementary relaxation times τ_i computed from Debye processes obtained by the FP procedure.

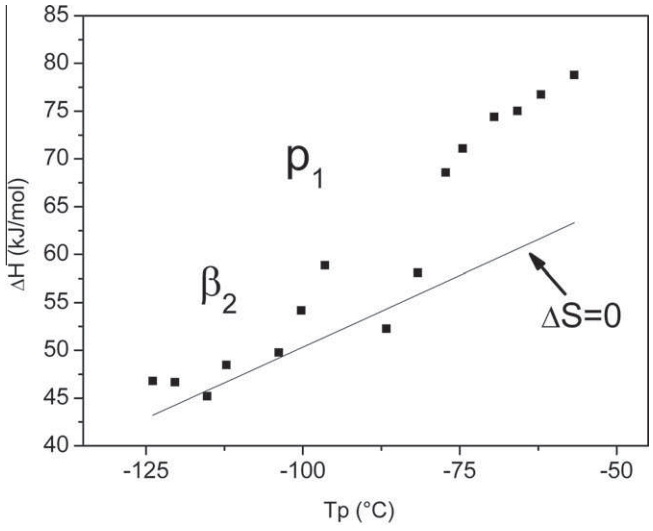

Fig. 9. Activation enthalpy of the elementary relaxation times τ_i of hydrated elastin ($h = 0.25$) deduced from the FP procedure as a function of the temperature of the peak. The Starkweather's function (Eq. (4)) corresponding to an equivalent frequency 10^{-3} Hz is superimposed on the figure as a continuous line.

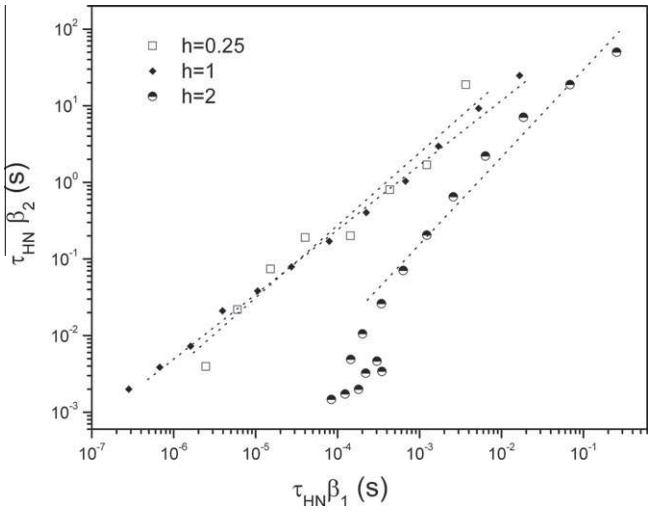

Fig. 10. Correlation between the relaxation times for β1 and β2 processes of elastin for various hydration levels.

3.2.3. Slower dynamics: p1 process

The p1 process observed by DDS is symmetrically broadened ($\beta \approx 1$, $0.77 < \alpha < 0.5$). Via the FP procedure, an increase of ΔH is observed for the p1 process, with values of ΔH between 55 and 75 kJ/mol as reported in Fig. 9. The relaxation processes becomes complex, involving cooperative motions of neighboring segments. If we plot the variation of $\log \tau_0$ versus ΔH, a linear law is observed for the points associated with the p1 process: $\log \tau_0 \cong -1977 - 2.11 \cdot 10^{-4} \Delta H$. Such a phenomenon, known as a compensation effect, was observed for hydrated elastin at $h = 1$ [23], on a larger range of enthalpies (up to 100 kJ/mol). In this case the dielectric peak was attributed to the relaxation of the complex elastin-bound water, that needs more energy to reorientate itself than free water and that must be a distributed relaxation, reflecting the distribution of water attachment sites along the polypeptidic chains, as already observed in hydrated keratins [51], hydrated collagen [52,53], water–methyl cellulose system [54] or of swollen polymers like PA, PVAc [55]. Previous dielectric works on hydrated proteins like lysozyme showed that bound water in this case behaves as a glassy system [56]; the large compensation observed for the p1 mode, with values of τ_0 and *Ea* reaching maxima generally observed for the dielectric manifestation of glass transition in polymers, could indicate a similar glassy behavior of bound water in elastin. As suggested in literature [57], this slower process could be attributed to the reorganization of the whole hydrogen-bond network, which affects rigidity, and hence, may be the α process. Finally, mechanical analysis of different elastin–polar solvent systems [34] evidenced such a relaxation mode, whom intensity and activation enthalpy increased with the size of the solvent (water, ethylene glycol and triethylene glycol were tested), confirming our assumption.

4. Conclusion

This study shows that the combination of both thermal analysis and dielectric techniques is useful to characterize a biopolymer in the hydrated state. The "filling" of the hydration shell of elastin is followed by DSC. The first hydration shell is completely "full" for 1.2–1.3 molecules of water bound to one elastin residue, when only non-freezable water covers the shell of the protein.

Localized motions (at the nanometric scale), undetectable by DSC, that occur at low temperature can be observed by the combined use of DDS and TSDC. In this case, the evolution of the local dipolar reorientations have been followed for different hydration contents, revealing an increasing complexity when coexist elastin, unfreezable water and freezable water. The fastest process β1 mode is attributed to reorientations of water in the hydration shell, needing the breaking of two hydrogen bonds ($\approx$50 kJ/mol) to occur. The assignment of the second fast process (β2 mode) is less obvious, as distinct interpretations are given in literature. In the case of hydrated elastin, this mode could be addressed to localized, non cooperative motions in the elastin/water system. A direct power law is evidenced between the relaxation time of the β1 mode and the β2 mode, leading us to conclude that the fast dynamics of water in the hydration shell drives the β2 one. So the dynamic nature of the hydration shell would lend significant mobility to the protein, as already observed in globular proteins.

These fast processes were shown non- or little cooperative when compared to the process p1, which is associated with more energetic (55–80 kJ/mol) and more cooperative motions in the elastin–water system.

These results on hydrated elastin are a basis to help to the question – How the solvent influences the protein dynamics – which still remains largely unanswered. Moreover, our experimental data could be useful for the assessment of starting conditions in molecular dynamics simulations: simulation on long polypeptidic sequences of elastin could be launched with a small hydration level, typically 10%, corresponding to detectable localized reorientations of the complex water/residues in dielectric spectroscopies.

At the present time we scanned the different kinds of mobility of hydrated elastin in the frozen state; the next step of the study will be performed at physiological temperature to follow the dynamics of hydrogen bonds network and protein, and to test in this case the two state model implying the dynamic exchange between bound and free water molecules [2].

References

[1] L. Zhang, Y.T. Kao, D. Zhong, J. Am. Chem. Soc. 131 (2009) 10677.
[2] N. Nandi, K. Bhattacharyva, B. Bagchi, Chem. Rev. 100 (2000) 2013.
[3] J. Sjostrom, J. Mattsson, R. Bergman, E. Johansson, K. Josefsson, D. Svantesson, J. Swenson, Phys. Chem. Chem. Phys. 12 (2010) 10452.
[4] S.A. Lusceac, M. Vogel, C.H. Herber, Biochim. Biophys. Acta 1804 (2010) 41.
[5] P.W. Fenimore, H. Frauenfelder, B.H. McMahon, R.D. Young, Proc. Natl. Acad. Sci. 101 (2004) 14408.
[6] H. Jansson, R. Bergman, J. Swenson, J. Phys. Chem. B 109 (2005) 24134.
[7] H. Frauenfelder, G. Chen, J. Berendzen, P.W. Fenimore, H. Jansson, B.H. McMahon, I.R. Stroe, J. Swenson, R.D. Young, Biophys. Comput. Biol. 106 (2008) 5129.
[8] H. Frauenfelder, Chem. Phys. 375 (2010) 612.
[9] S.A. Lusceac, M. Rosenthil, M. Vogel, C. Gainaru, A. Fillmer, R. Bohmer, J. Non-Cryst. Solids 357 (2010) 655.
[10] K.L. Ngai, S. Capaccioli, N. Shinyashiki, J. Phys. Chem. B 112 (2008) 3826.
[11] E.G. Cleary, M.A. Gibson, in: W.D. Comper (Ed.), Extracellular Matrix, vol. 2, Harwood Academic Publishers, Melbourne, 1996, p. 95.
[12] J.A. Foster, L. Rubin, H.M. Kagan, C. Franzblau, E. Bruenger, L.B. Sandberg, J. Biol. Chem. 249 (1974) 6191.
[13] L.B. Sandberg, J.M. Davidson, Peptide Prot. Rev. 3 (1984) 169.
[14] D.W. Urry, J. Prot. Chem. 3 (1984) 403.
[15] L. Debelle, A.M. Tamburro, Int. J. Biochem. Cell. Biol. 31 (1999) 261.
[16] A.M. Tamburro, A. Pepe, B. Bochicchio, Biochemistry 45 (2006) 9518.
[17] A.M. Tamburro, B. Bochicchio, A. Pepe, Biochemistry 42 (2003) 13347.
[18] J.P. Mackay, L.D. Muiznieks, P. Toonkool, A.S. Weiss, J. Struct. Biol. 150 (2005) 154.
[19] N. Floquet, S. Héry-Huynh, M. Dauchez, P. Derreumaux, A.M. Tamburro, A.J. Alix, Biopolymers 76 (2004) 266.
[20] B. Li, V. Daggett, J. Muscle Res. Cell. Motility 23 (2002) 561.
[21] P. Papadopoulos, G. Floudas, H.A. Klok, I. Schnell, T. Pakula, Biomacromolecules 5 (2004) 81.
[22] V. Samouillan, A. Lamure, C. Lacabanne, Chem. Phys. 255 (2000) 259.
[23] V. Samouillan, C. André, J. Dandurand, C. Lacabanne, Biomacromolecules 5 (2004) 958.
[24] C. Gainaru, A. Fillmer, R. Böhmer, J. Phys. Chem. B 113 (2009) 12628.
[25] D. Tintar, V. Samouillan, J. Dandurand, C. Lacabanne, A. Pepe, B. Bochicchio, A.M. Tamburro, Biopolymers 91 (2009) 943.
[26] A.I. Lansing, T.B. Rosenthel, M. Alex, E.W. Dempsey, Anat. Rec. 114 (1952) 555.

[27] G. Teyssedre, S. Mezghani, A. Bernes, C. Lacabanne, in: J.F. Runt, J.J. Fitzgerald (Eds.), Dielectric Spectroscopy of Polymeric Materials. Fundamental and Applications, ACS, Washington, DC, 1997, p. 227.
[28] J. Rault, A. Lucas, R. Neffati, M. Monleon Pradas, Macromolecules 30 (1997) 7866.
[29] T. Kaasgaard, O.G. Mouritsen, K. Jorgensen, Biophys. Biochim. Acta 1615 (2003) 77.
[30] L.B. Sandberg, Int. Rev. Connect. Tissue Res. 7 (1976) 159.
[31] G. Cecorrulli, M. Scandola, G. Pezzin, Biopolymers 16 (1977) 1505.
[32] A. Perry, M.P. Stypa, B.K. Tenn, K.K. Kumashiro, Biophys. J. 82 (2002) 1086.
[33] L. Gotte, M. Mammi, G. Pezzin, in: W.G. Grewther (Ed.), Symposium on Fibrous Proteins, vol. 1, Butterworth, Sydney, 1968, p. 236.
[34] J. Swenson, H. Jansson, J. Hedström, R. Bergman, J. Phys.: Condens. Matter 19 (2007) 205109.
[35] S. Havriliak, S. Negami, Polymer 8 (1967) 161.
[36] M.E. Brown, P. Kent Gallagher, in: Handbook of Thermal Analysis and Calorimetry: Recent Advances, Techniques and Applications, Elsevier, Amsterdam, 2008, p. 253.
[37] V. Samouillan, Thesis of Paul Sabatier University, S.N. 3455, Toulouse, France, 1999.
[38] J. Mijovic, Y. Bian, R.A. Gross, B. Chen, Macromolecules 38 (2005) 10812.
[39] S. Cerveny, A. Alegria, J. Colmenero, Phys. Rev. E 77 (2008). 031803-1.
[40] S. Sudo, S. Yagihara, J. Phys. Chem. B 113 (2009) 11448.
[41] H. Vogel, Phys. Z. 22 (1921) 645.
[42] S.J. Suresh, V.M. Naik, J. Chem. Phys. 113 (2000) 9727.
[43] S. Cerveny, G.A. Schwartz, R. Bergman, J. Swenson, J. Phys. Rev. Lett. 93 (2004) 245702.
[44] B. Geil, T.M. Kirschgen, F. Fujara, Phys. Rev. B 72 (2005) 014304.
[45] G.P. Johari, E. Whalley, J. Chem. Phys. 75 (1981) 1333.
[46] S.J. Kawada, J. Phys. Soc. Jpn. 44 (1978) 1881.
[47] R.E. Grimm, D.E. Stillman, S.F. Dec, M. Bullock, J. Phys. Chem. B 112 (2008) 15382.
[48] V. Samouillan, J. Dandurand, C. Lacabanne, W. Hornebeck, Biomacromolecules 3 (2002) 531.
[49] C. Bucci, R. Fieshi, G. Guidi, Phys. Rev. 148 (1966) 816.
[50] W. Starkweather, Macromolecules 14 (1981) 1277.
[51] J.L. Leveque, J.C. Garson, P. Pissis, G. Boudouris, Biopolymers 20 (1981) 2649.
[52] S. Nomura, A. Hiltner, J.B. Lando, E. Baer, Biopolymers 16 (1977) 231.
[53] H. Maeda, E. Fukada, Biopolymers 21 (1982) 2055.
[54] P. Pissis, D. Daoukaki-Daimanti, Chem. Phys. 123 (1988) 165.
[55] H.M. Le Huy, J. Rault, Polymer 35 (1994) 136.
[56] M. Peyrard, Phys. Rev. E 64 (2001) 11109.
[57] M. Vogel, Phys. Rev. Lett. 101 (2008) 225701.